Dopants for independent control of precessional frequency and damping in $Ni_{81}Fe_{19}$ (50 nm) thin films

S. G. Reidy, L. Cheng, and W. E. Bailey[a)]
Materials Science Program, Department of Applied Physics, 200 S.W. Mudd Bldg., 500 West 120th Street, Columbia University, New York, New York 10027

(Received 21 October 2002; accepted 18 December 2002)

Dilute impurities can be used to control the dynamical response of ferromagnetic thin film magnetization at frequencies >1 GHz. Central lanthanide dopants (Sm, Eu, Tb, Dy, and Ho) have been investigated for their effect on the magnetization dynamics of $Ni_{81}Fe_{19}$ (50 nm). We find that Sm, Dy, and Ho contribute an increase on damping α up to four times stronger per concentration than that provided by Tb, with minimal effect on precessional frequency. One dopant, Eu, leaves α unchanged but boosts the resonant frequency f_p of the system by ~500 MHz for 3% addition, equivalent to a dynamic anisotropy field of 9 Oe, ''stiffening'' the system. The results indicate that precessional frequency and damping may be controlled independently in magnetoelectronic device materials. [DOI: 10.1063/1.1544642]

The high-speed response of magnetoelectronic devices (>1 GHz) rests on the dynamical response of ultrathin film magnetization. Two key materials parameters that control the response, according to the Landau–Lifshitz or–Gilbert equations (LLG), are the damping/spin relaxation rate λ_{LL} (s^{-1}) and dynamic anisotropy field H_K. While significant recent effort has gone into extracting these parameters from ultrafast (ps) time-domain measurement,[1–4] relatively little modern work exists on their materials-based control or underpinnings.

Dilute concentrations (''dopants'') of the rare-earth (RE) element Tb have been found recently to be very effective in manipulating α of $Ni_{81}Fe_{19}$.[5] In this letter, we show that the contributed damping varies systematically across the central portion of the lanthanide series Sm–Ho, indicating a strong apparent correlation to the magnetic state of the RE. Effects of some species are several times greater than those observed presently for Tb. Furthermore, we show that Eu dopants offer control over the dynamic anisotropy field H_K *without* effect on damping; 2.7% of Eu ''stiffens'' the system equivalently to anisotropy of 9 Oe, increasing the precessional frequency f_p by ~500 MHz. The results suggest that induced relaxation in RE-doped $Ni_{81}Fe_{19}$ correlates well with the magnetic state of the RE, and that ω_p and relaxation α can be selected independently in magnetoelectronic device materials.

RE-doped $Ni_{81}Fe_{19}$ (50-nm) thin films were prepared using ion-beam deposition in a load-locked, production-oriented chamber (Veeco Millatron). Dopants were introduced into the films by cosputtering with thin foils of the RE, mounted on a manipulator that could be positioned in and out of the beam. Electromagnet-induced bias of approximately 20 Oe was applied to enhance uniaxial anisotropy.

The dopant concentration of the film x, creating composition $(Ni_{81}Fe_{19})_{1-x}RE_x$, was adjusted by raising or lowering the foil into/out of the beam prior to film deposition. Films of $(Ni_{81}Fe_{19})_{1-x}RE_x$ (RE=Sm, Eu, Tb, Dy, and Ho) were investigated in the study. Increased damping was observed in all series (except Eu, to be described) for increasing positioning of the foil into the beam. To control for possible *ex situ* surface oxidation of the RE foil targets, foils were presputtered iteratively up to 10 h until consistent dynamical characteristics were obtained for doped films. Films with gross similarity in damping were selected for compositional analysis using x-ray photoelectron spectroscopy (XPS), provided by a separate load-locked PHI 550 spectrometer. A low-energy Ar sputter clean was applied *in situ* to remove the surface oxide of the $Ni_{81}Fe_{19}$:RE prior to analysis.

Magnetization dynamics of the thin films were characterized using a time-domain pulsed inductive technique. Measured wave forms are proportional to $\partial\phi/\partial t(t)$, where ϕ is the in-plane angle of the magnetization with respect to the bias field. See Refs. 1 and 5 for details. Magnetic field bias H_B is applied along the easy-axis direction, orthogonal to the pulsed field; $H_B=20$ Oe unless noted otherwise. Measurements were taken at room temperature.

Experimental measurements of magnetization dynamics were fit to the numerically integrated full-angle LL equation, including thin-film demagnetizing, anisotropy, and bias fields in H_{eff}. M_s was set to the literature value for undoped $Ni_{81}Fe_{19}$, 730 kA/m, H_p to the nominal value of 18 Oe. Fit parameters were constrained to the anisotropy field H_K, the LL relaxation rate λ, and the inductive coupling efficiency ν, which scales only the magnitude of the observed voltage. LLG fits were carried out in comparison; we find that the two model predictions of $\theta(t)$ and $\phi(t)$ agree to better than 1% numerical accuracy up to $\lambda/4\pi=2.5$ GHz ($\alpha=0.3$), as expected in the regime $\alpha\ll1$.

Representative experimental measurements of magnetization dynamics are shown, with LL/LLG fits, in Fig. 1 for the case of the $Ni_{81}Fe_{19}$:Dy system, $0<x_{Dy}<6\%$. Full-angle, numerically integrated LL/LLG fitted values of λ, expressed as $\lambda/4\pi$, are listed in the fits; these can be compared visually with the ''ring-down time'' τ, in which the damping term in $V_{ind}(t)$ takes the form $e^{-t/\tau}$, and $\lambda=2/\tau$. Agreement between the model and experiment is close except in the case

a)Electronic mail: web54@columbia.edu

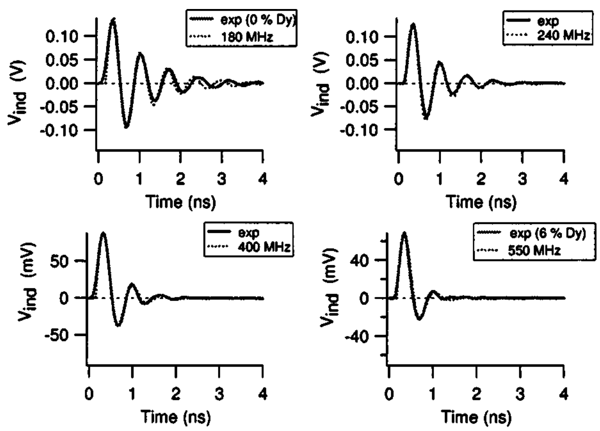

FIG. 1. Inductive response [voltage $V_{ind}(t)$] for a series of Dy-doped $Ni_{81}Fe_{19}$ films, increasing doping $0\% < x_{Dy} < 6\%$. LL/LLG fits and estimated values of $\lambda/4\pi$ are shown. There is an evident increase in relaxation rate λ with composition, spanning $180 < \lambda/4\pi < 550$ MHz $(0.014 < \alpha < 0.043)$.

of undoped $Ni_{81}Fe_{19}$, in which some evident shift in the frequency appears at longer times (3 ns). H_K is set to 5–6 Oe in all fits except Eu according to $\omega_p(H_B)$ measurements (to be discussed).

It is evident that the Dy doping series, formed by ion-beam deposition, spans underdamped to nearly critically damped dynamics. This range of moderate effects is of great interest for applications, and had not been attainable through cosputtering elemental targets of Tb and $Ni_{81}Fe_{19}$. Compositional analysis of the most heavily Dy-doped film, with $\lambda/4\pi = 550$ MHz (bottom right, Fig. 1), by XPS yields $x_{Dy} = 5.2 \pm 1.5\%$.

To yield an estimate of contributed damping per atomic percentage of the RE dopant, we make two assumptions. First, relaxation rates of the undoped film are assumed to sum with the contributed effects of the dopant. This approach can be justified through different temperature-dependent relaxation behavior $[\alpha = \alpha(T)]$ found for undoped and 2% Tb-doped films: weak and positive for undoped films, and strong and negative for Tb-doped films. Secondly, we assume that the contributed damping is proportional to atomic percentage of RE in the dilute doping regime, as found previously for Tb.[5] We then find $(\lambda/4\pi)/(a/o_{Dy}) = (550-180)$ MHz/5.2 $\pm 1.5\%$, or $\lambda/(\%_{Dy}) = 890 \pm 260$ MHz.

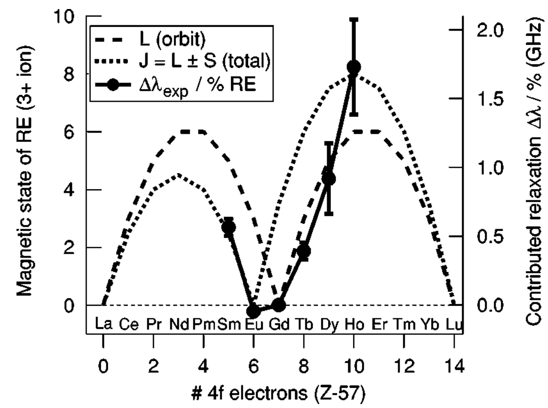

FIG. 3. Contributed damping to $Ni_{81}Fe_{19}$ as a function of lanthanide dopant atomic number $Z-57$ (La=57). The angular momentum states of the isolated dopants are shown for comparison.

This analysis has been applied additionally to Sm, Eu, Tb, and Ho. Analogous effects are shown except in the case of Eu, in which no damping is contributed. The data and fits are shown in Fig. 2. Good agreement is again found between model and experiment, although the fit quality is poorer for the case of Sm- and Ho-doped films.

The comparison of contributed relaxation rate across the central portion of the lanthanide series, $\lambda/(\%_{RE})(Z)$, is presented in Fig. 3. We find a roughly V-shaped dependence of contributed damping for these elements, with zeroes corresponding to Eu and Gd (point taken from Ref. 5). The theoretical orbital and total angular momentum numbers L and J are plotted for comparison. The zero in contributed damping corresponds to zeroes in L and J expected for the $4f$ shell.

Eu doping (3%) increases the resonant frequency of the system *without* contributing relaxation. Comparing the response in Fig. 1 (top left) with that in Fig. 2 (top left) reveals six maxima in the latter case and five in the former for $H_B = 20$ Oe. More quantitative measurement of resonant frequency $f_p(=\omega_p/2\pi)$ is found through a Fourier transform of the data, appropriate for the low relaxation rates of $\lambda/4\pi = 160$ and 180 MHz, found respectively for Eu-doped and undoped $Ni_{81}Fe_{19}$.

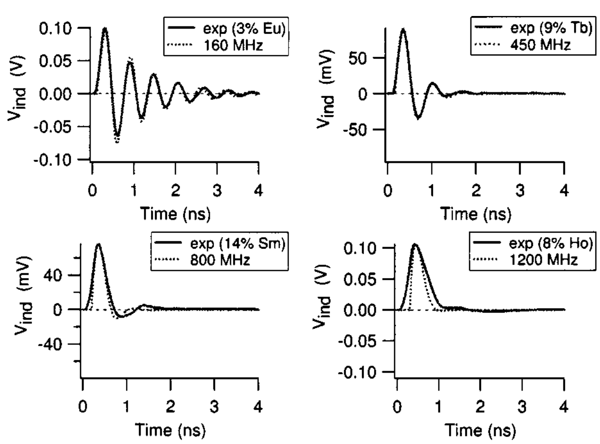

FIG. 2. Comparable fits for representative members of the Eu, Sm, Tb, and Ho series, with composition characterized by XPS. Strong effects on damping are observed for all dopants except Eu.

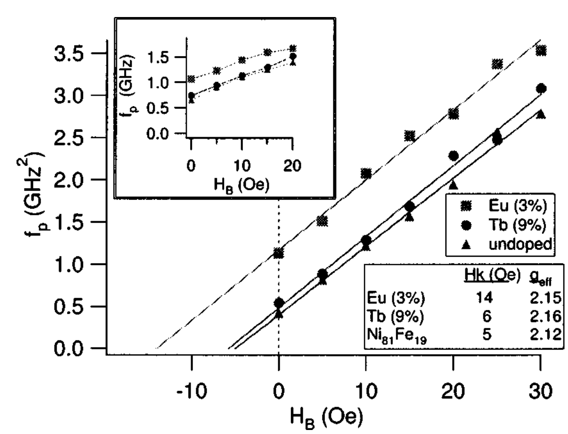

FIG. 4. Kittel plot for undoped, Tb-doped, and Eu-doped $Ni_{81}Fe_{19}$, longitudinal bias. Inset, left: ω_P vs bias field H_B. Table, right: extracted values of dynamic H_K and g-factor. Note the 9 Oe enhancement of dynamic H_K provided by Eu.

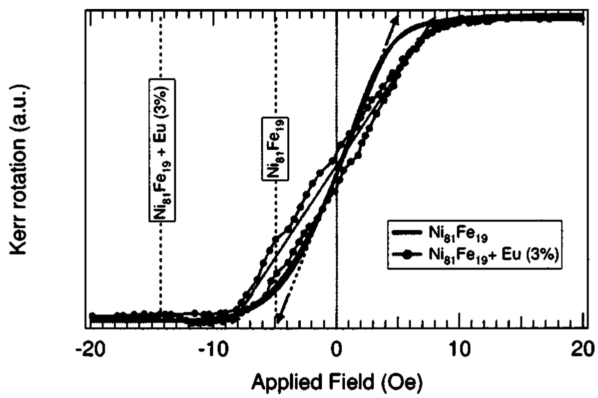

FIG. 5. MOKE hard-axis hysteresis loops for undoped and Eu-doped $Ni_{81}Fe_{19}$; dynamic H_k values are shown for comparison.

Figure 4 shows the bias field dependence of f_p, plotted as $f_p^2(H_B)$ to compare with the Kittel relation,

$$f_p^2=\left(\frac{\omega_P}{2\pi}\right)^2\simeq\frac{\gamma^2\mu_0^2M_s}{4\pi^2}(H_K+H_B),$$

for in-plane ferromagnetic resonance (FMR) in a thin film, where the prefactor evaluates to $0.07199(g_{\text{eff}}/2)^2\text{GHz}^2/\text{Oe}$. We use this relationship to extract dynamic anisotropy fields H_K and the $g_{\text{eff}}^2M_s$ product for the films. Marked differences are found in the dynamic anisotropy field H_K: 5 Oe$\pm$1 Oe for undoped and Tb-doped films, but 14$\pm$1 Oe for 3% Eu-doped. This corresponds to a boost in resonant frequency by 480 MHz without increase in loss. The result found for Eu-doped $Ni_{81}Fe_{19}$ is significant to the extent that other materials techniques are not well known which can enhance ω_p without increasing dissipation.

Essentially constant values of $g_{\text{eff}}^2M_s$ are found within experimental error. Assuming that M_s remains constant at 730 kA/m, we have $g_{\text{eff}}=2.16\pm0.05$ for Eu 3%, 2.15 $\pm$0.05 for Tb 9%, and 2.12$\pm$0.05 for $Ni_{81}Fe_{19}$, consistent with the value of 2.07 found previously.[1] We note furthermore that the fitted value of α is essentially constant for applied bias $H_B>5$ Oe for Eu-doped and 10 Oe for undoped or Dy-doped films, providing some justification for the use of the Gilbert damping form. Comparison of measured dynamic H_k with static H_k, as measured by magneto-optical Kerr expect (MOKE) (Fig. 5), shows good agreement for undoped $Ni_{81}Fe_{19}$, but a much larger dynamic H_K for the Eu-doped case by nearly a factor of two.

Some of our observations on dynamics of RE-doped $Ni_{81}Fe_{19}$ are consistent with 1960s' observations on FMR of RE-substituted YIG.[6] RE species are thought to contribute damping in YIG by coupling the magnetization to the lattice through the orbital moment. Negligible contributed damping in Eu:YIG and Gd:YIG had been attributed to the nonmagnetic ground state of Eu ($J_{\text{Eu}}=0$) and the absence of an orbital moment in Gd ($L_{\text{Gd}}=0$), respectively.[7] A strong, growth-induced anisotropy has also been observed in substituted europium iron garnet, absent in gadolinium iron garnet.[8] These similarities suggest that the properties of doped films arise from the magnetic properties of the isolated RE elements.

However, the trend in contributed damping versus Z ($\lambda/\%_{\text{RE}}$) differs strongly from YIG results, which peak strongly at Tb in YIG; this behavior indicates some matrix dependence of the effects of REs, and is presently unexplained. We hope that the results will stimulate some theoretical interest, and offer additional degrees of freedom in engineering the gigahertz response in magnetoelectronic devices.

We thank A. Kos for use of his original computer code in the pulsed inductive measurement system. This work was supported in part by the MRSEC Program of the National Science Foundation under Award Number DMR-0213574. We acknowledge the support of the Army Research Office under Grant ARO-43986-MS-YIP and the NIST Nanomagnetodynamics program, Grant 60NANB2D0145.

[1] T. Silva, C. Lee, T. Crawford, and C. Rogers, J. Appl. Phys. **85**, 7849 (1999).
[2] S. E. Russek, S. Kaka, and M. J. Donahue, J. Appl. Phys. **87**, 7070 (2000).
[3] C. Back, R. Allenspach, W. Weber, S. S. P. Parkin, D. Weller, E. L. Garwin, and H. C. Siegmann, Science **285**, 864 (1999).
[4] R. Koch, G. Grinstein, G. Keefe, Y. Lu, P. Troulloud, W. Gallagher, and S. Parkin, Phys. Rev. Lett. **84**, 5419 (2000).
[5] W. Bailey, P. Kabos, F. Mancoff, and S. Russek, IEEE Trans. Magn. **37**, 1749 (2001).
[6] M. Sparks, *Ferromagnetic-Relaxation Theory* (McGraw-Hill, New York, 1964).
[7] P. Seiden, Phys. Rev. **133**, A728 (1964).
[8] M. Sturge, R. LeCraw, R. Pierce, S. Licht, and L. Shick, Phys. Rev. B **7**, 1070 (1973).